The Astrophysical Journal Supplement Series, 223:12 (11pp), 2016 March doi:10.3847/0067-0049/223/1/12

THE SPECTRUM AND TERM ANALYSIS OF Co III MEASURED USING FOURIER TRANSFORM AND GRATING SPECTROSCOPY

D. G. Smillie[1], J. C. Pickering[1], G. Nave[2], and P. L. Smith[3]
[1] Blackett Laboratory, Imperial College London, London SW7 2AZ, UK; j.pickering@imperial.ac.uk
[2] National Institute of Standards and Technology, Gaithersburg, MD 20899-8422, USA
[3] Harvard-Smithsonian Center for Astrophysics, 60 Garden Street, Cambridge, MA 02138, USA
Received 2015 June 16; accepted 2015 December 2; published 2016 March 29

ABSTRACT

The spectrum of Co III has been recorded in the region 1562–2564 Å (64,000 cm^{-1}–39,000 cm^{-1}) by Fourier transform (FT) spectroscopy, and in the region 1317–2500 Å (164,000 cm^{-1}–40,000 cm^{-1}) using a 10.7 m grating spectrograph with phosphor image plate detectors. The spectrum was excited in a cobalt–neon Penning discharge lamp. We classified 514 Co III lines measured using FT spectroscopy, the strongest having wavenumber uncertainties approaching 0.004 cm^{-1} (approximately 0.2 mÅ at 2000 Å, or 1 part in 10^7), and 240 lines measured with grating spectroscopy with uncertainties between 5 and 10 mÅ. The wavelength calibration of 790 lines of Raassen & Ortí Ortin and 87 lines from Shenstone has been revised and combined with our measurements to optimize the values of all but one of the 288 previously reported energy levels. Order of magnitude reductions in uncertainty for almost two-thirds of the $3d^64s$ and almost half of the $3d^64p$ revised energy levels are obtained. Ritz wavelengths have been calculated for an additional 100 forbidden lines. Eigenvector percentage compositions for the energy levels and predicted oscillator strengths have been calculated using the Cowan code.

Key words: atomic data – line: identification – line: profiles – methods: laboratory: atomic

Supporting material: machine-readable tables

1. INTRODUCTION

Modern space- and ground-based spectrographs have yielded dramatic improvements in the resolution and accuracy of observed stellar spectra in the past few decades. Deficiencies in the laboratory-measured atomic data necessary to fully interpret such spectra have been exposed: transition wavelengths, previously uncertain by 5 mÅ at best, must be known to a few parts in 10^7, or approximately 0.2–0.5 mÅ in the vacuum ultraviolet region (VUV, wavelengths shorter than 2000 Å) (Pickering 2002). Accurate energy levels must be established to calculate transition wavelengths for lines that are not observed in the laboratory because they are blended, outside the measurement range, or forbidden but observed in astronomical spectra (Leckrone et al. 1996; Smith et al. 1998). Much of observed stellar opacity is due to the astrophysically important iron group elements (Johansson 1987), with the VUV spectra of hot B stars, in particular, dominated by the doubly ionized iron group elements (Swings et al. 1976; Cowley & Frey 1988). Existing published atomic data (transition wavelengths and energy levels) for the doubly ionized iron group elements fall far short of the uncertainty requirements for analyzing modern stellar spectra; in many cases, greater than order of magnitude improvements in wavelength and energy level accuracies are needed (Pickering 2002).

Fourier transform (FT) spectroscopy combines a large free spectral range with high resolution for accurate measurements of atomic spectra. Using this technique, much progress has been made toward improving knowledge of the neutral and singly ionized iron group spectra; see, for example: V I (Thorne et al. 2011); V II (Thorne et al. 2013); Cr I (Murray 1992); Fe I (Nave et al. 1994); Fe II (Nave & Johansson 2013); Co I (Pickering & Thorne 1996); and Co II (Pickering et al. 1998). With the use of a Penning discharge lamp (PDL), measurements using a Fourier transform spectrometer (FTS) now include the doubly ionized iron group spectra (Smith et al. 1998; Smillie et al. 2006, 2008). The work discussed herein presents the first FTS measurements of the Co III spectrum. Supplementing the FTS measurements are grating spectrometer measurements, using the normal incidence vacuum spectrograph (NIVS; Nave et al. 2011) at the US National Institute of Standards and Technology (NIST) for wavelengths below the FTS short wavelength cut-off (1400 Å) and for studying weaker lines at longer wavelengths. Improved values of 287 Co III energy levels are given.

The major compilations of energy levels for the doubly ionized iron group elements are found in Moore (1952) and (Sugar & Corliss 1985, hereinafter S&C). The only analysis of Co III included in Moore (1952) was the unpublished work by Shenstone, which he considerably extended and subsequently published in Shenstone (1960). He measured the spectrum in the region 650–3800 Å and established 213 levels of the $3d^7$, $3d^64s$, $3d^64p$, $3d^64d$, and $3d^65s$ configurations with an uncertainty presumed in S&C to be 0.5 cm^{-1}. Energy level eigenvector percentage compositions were calculated by Pasternak & Goldschmidt (1972) for the $3d^7$ configuration, Vizbaraite et al. (1968) for the $3d^64s$ configuration and Roth (1968) for the $3d^64p$ configuration. The most recent experimental measurements of Co III were undertaken by Raassen & Ortı Ortin (1984, hereinafter R&O), who analyzed the three lowest configurations: $3d^7$, $3d^64s$, and $3d^64p$. They measured the spectrum in the range 450–3100 Å, with hollow cathode and sliding spark sources using grating spectrographs. They established all 19 possible levels of the $3d^7$ configuration, 58 out of a possible 63 levels for the $3d^64s$ configuration, and 178 out of a possible 180 levels for the $3d^64p$ configuration (S&C established 17, 41, and 122 levels, respectively), finding 8 of Shenstone's $3d^64p$ level values erroneous. The R&O energy level uncertainties are given as 0.5 cm^{-1} for the $3d^7$ levels and

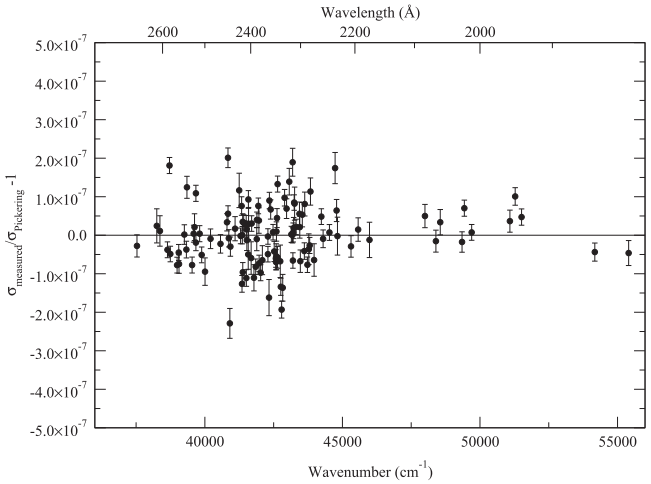

Figure 1. Comparison between the standard line and measured line wavenumbers for the FTS cobalt–neon PDL spectrum, after application of the wavenumber correction to the entire spectrum. The error bars are the uncertainties of the new FTS spectrum only.

0.2 cm^{-1} for the $3d^64s$ levels (and, we assume, 0.2 cm^{-1} for the $3d^64p$ levels as well). These energy levels were established using 1310 transition lines with uncertainties of 5 mÅ for the $3d^7$–$3d^64p$ transitions and 10 mÅ for the $3d^64s$–$3d^64p$ transitions. Using the method outlined in Hansen & Raassen (1981), R&O also calculated level eigenvector percentage compositions for the levels of the three configurations, although they favor Roth's calculations for their level values at 126,999.6 and 127,052.3 cm^{-1}.

The strongest lines from our FTS measurements have a wavenumber (σ) uncertainty of 0.004 cm^{-1} (approximately 0.2 mÅ at 2000 Å), greater than an order of magnitude improvement over previous measurements, and are now at the level of uncertainty required for analysis of modern stellar spectra such as the spectra being recorded in the ASTRAL II program with the *Hubble Space Telescope* (*HST*; Ayres 2013). Our Co III lines measured using grating spectroscopy have a range of uncertainties similar to those of R&O (approximately 5–10 mÅ). The revised energy level values are presented, together with Ritz wavelengths, calculated transition oscillator strengths, and level eigenvector percentage compositions.

2. EXPERIMENTAL DETAILS

A PDL designed by Heise et al. (1994) was used to excite the energy levels of Co III for all our measurements. Pure (+99.9%) cobalt cathodes and ultra high purity neon buffer gas were used. The best excitation of the doubly ionized spectrum is achieved by running the PDL at the highest currents and lowest pressures at which a stable discharge can be maintained for 1–2 hr. Good excitation of Co III was obtained using discharge currents of 1.75 A and 1.6 A for the FTS and grating measurements, respectively, with buffer gas pressures of approximately 0.1–0.2 Pa ((1 to 2) $\times 10^{-3}$ mbar). The dominant ionization stage, however, remained Co II. The discharge voltages were in the range 1.00–1.15 kV.

2.1. FTS Measurements

The spectrum of Co III was measured in the wavenumber region 33,000–66,000 cm^{-1} (3030–1515 Å) using the NIST VUV FTS (Griesmann et al. 1999) (Spectrum number 6, taken on 1999 August 30). Hamamatsu R7154 photomultiplier detectors[4] were used on each of the two outputs, and 80 scans were co-added to increase the signal-to-noise ratio (S/N) of the spectral lines. A resolution of 0.2 cm^{-1} was used, which fully resolved the Co III line profiles. Because of hyperfine structure (HFS), the average full width at half maximum (FWHM) of 0.78 cm^{-1} (0.031 Å at 2000 Å) is much broader than for Cr III lines excited by a PDL (Smillie et al. 2008) with average Cr III line FWHM of 0.28 cm^{-1} (0.011 Å at 2000 Å); the Co III lines also exhibit a greater range in FWHM (with a standard deviation of 0.27 cm^{-1} compared with 0.06 cm^{-1} for the Cr III lines).

A spectrum of a radiometrically calibrated deuterium lamp (Cathodeon Ltd V04 (see footnote 4) calibrated at the Physikalisch-Technische Bundesanstalt (PTB) synchrotron in the range 164–300 nm (Hollandt et al. 2000)) was recorded after the PDL spectrum was taken. It was used to determine the instrument response function for the FTS measurements by dividing the recorded spectrum by the calibrated radiance. Relative intensities of the Co III lines were obtained by dividing the measured integrated intensity of the line by the instrumental response function.

Analysis of the observed FTS spectrum was carried out using the XGREMLIN program (Nave et al. 1997, 2015). The resulting line list was comprised of: wavenumber (wavelength), the S/N, the full width at half-maximum (FWHM) of the line, and the integrated intensity. Because of the broadening effect of HFS, the line profiles cannot be fitted with a Voigt profile, so the wavenumber was determined from the center of gravity (COG) of the area under the line profile. The wavenumber uncertainty for a COG fit is approximately given by the FWHM of the line divided by twice the S/N, although may be larger for the weaker lines (Pickering & Thorne 1996).

The wavenumber calibration of the FTS spectrum was carried out using reference wavenumbers of Co I and Co II taken from FTS measurements of the cobalt–neon hollow cathode lamp spectrum (Pickering 1994; Pickering & Thorne 1996; Pickering et al. 1998). We selected strong isolated spectral lines from these measurements with an uncertainty of 0.004 cm^{-1} (approximately 0.2 mÅ at 2000 Å). The reference wavenumbers were originally calibrated using the Ar II wavenumber standards of Norlén (1973), which were subsequently shown to be too small by 6.7 parts in 10^8 (Whaling et al. 1995; Nave & Sansonetti 2011). We thus increased the wavenumbers of the reference lines to put them on the same scale as the Ar II wavenumbers of Whaling et al. (1995). All of the Co I and Co II reference lines with a S/N greater than 100 in our spectra were used to derive a wavenumber correction factor. The ratio between the reference wavenumbers and our wavenumbers after application of this correction factor is shown in Figure 1. The total wavenumber uncertainty for our measurements depends on the wavenumber calibration and the line fitting uncertainties, with the wavenumber uncertainty of our strong isolated spectral lines approaching the uncertainty of the wavelength standard lines of approximately 0.004 cm^{-1} for one standard uncertainty.

[4] Certain commercial equipment is identified in this article to adequately specify the experimental procedure. Such identification does not imply endorsement by the National Institute of Standards and Technology, nor does it imply that this equipment is the best available for the purpose.

2.2. Grating Measurements

The Co III spectrum was also observed in the region 234–2550 Å with the 10.7 m NIST NIVS (two spectra named x872 and x875, recorded on 2005 May 26, and June 8, respectively). However, our spectra were not a significant improvement over previous measurements for wavelengths below 1200 Å. A gold coated grating, 1200 lines per mm, blazed at 1200 Å was used at angles of incidence from 4° to 10°.

The spectra were recorded on Fuji BAS-TR 2040 image plates (see footnote 4) measuring about 5 cm × 25 cm. These plates do not have a protective coating over the phosphor that would absorb UV light. Three plates were used for each spectrum, producing a total wavelength coverage of about 600 Å. The image plates were read with a rotary drum scanner (PerkinElmer Cyclone Storage Phosphor Scanner B41200 (see footnote 4)), which illuminates the plate with red light from a laser, while a photomultiplier tube detects the blue light emitted through photostimulated luminescence (Katto et al. 1993; Iwabuchi et al. 1994). The grating slit width used, 52 μm, was selected due to the inherent resolution limitation imposed by the scanner (pixel size ~42 μm). A scan is completed within a few minutes and the image is stored as a TIFF (Tagged Image File Format). In several cases, strong lines saturated the detector in the image plate scanner. Successive scans of the plate were used to mitigate the saturation and thereby extend the effective dynamic range (Nave et al. 2011).

Spectra for analysis were extracted from the digital image by integrating each spectrum across the full height of the image of the slit, taking into account any slope of the image relative to the plate, and saving the result as a two column text file of position and signal (Smillie 2007). Care was taken to ensure that the signal was integrated over the same number of pixels for each data point in the spectrum, in both the spectrum of interest and the corresponding spectrum of the deuterium lamp used for intensity calibration. Analysis of the observed grating spectra was also carried out using the XGREMLIN program, resulting in a line list with the same parameters as discussed above for the FTS spectrum. Voigt profiles were fitted to the lines and the residuals were of the same order as the background noise in the majority of cases.

The typical linewidths on the phosphor image plates are about 0.1 Å and are determined by the resolution of the scanner. Although this is much larger than obtainable with a photographic plate, the linearity of the phosphor image plates means that the center of the line can be obtained with an uncertainty of about 0.005 Å, which is similar to that obtainable from photographic plates (Reader et al. 2006).

Wavelengths of lines in the grating spectra were calibrated using lines from our FTS cobalt–neon PDL spectrum as standards for wavelengths longer than approximately 1600 Å. The calibration was extended down to 1150 Å using Co II Ritz wavelengths (i.e., those calculated from experimentally determined energy levels) determined from the energy levels in Pickering (1998) and Pickering et al. (1998), and some Co II observed wavelengths from Iglesias (1979). The NIST NIVS dispersion gives a plate factor of 0.078 nm mm^{-1} in the first order, and is approximately linear, although a high order polynomial fit is necessary. A polynomial was fitted to the difference between the wavelength derived from a linear dispersion and the wavelength standards, weighted by the fitting uncertainties of the measured lines. The order of the polynomial fit was automatically varied between 1 and 15, with the order producing the lowest standard uncertainty chosen for the final calibration. Full details of the polynomial fits and standard lines can be found in (Smillie 2007). For most of the spectra, the standard lines were well distributed throughout the spectral range (average of 5 standard lines per nm), allowing local plate deviations to be accounted for. Any lines in spectral regions where this was not the case were not included in the final line list or in the energy level fitting. Wavelengths of spectral lines recorded in more than one spectrum were averaged. Uncertainties (one standard uncertainty) due to the wavelength calibration are estimated to be approximately 3–4 mÅ. A typical dispersion curve and residuals after the fit are shown in Figure 2 for the 1790–1980 Å region; additional examples are given in (Smillie 2007).

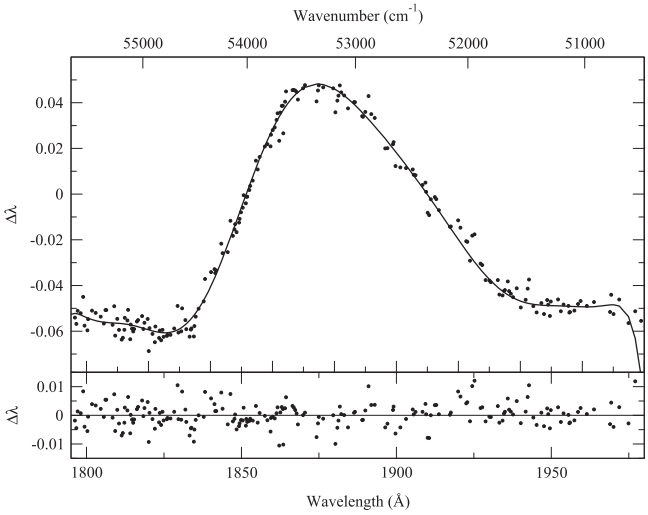

Figure 2. Top: difference between wavelength derived from a linear dispersion and the actual standard wavelengths ($\Delta\lambda$) as a function of wavelength λ. Bottom: residuals after fitting a 12th order polynomial to the data.

Deuterium lamp spectra were also recorded down to approximately 1150 Å. For spectra recorded in both FTS and grating spectra the intensities of the lines measured in the grating spectra were adjusted to the intensity scale of the FTS spectra. For wavelengths below 1600 Å there were no overlapping spectra and the grating intensities were scaled to put them on a consistent scale using our calculated oscillator strengths (see Section 3.2). The intensities of lines measured in both FTS and grating spectra agree to about 20%. However, because we could not ensure that either the FTS or the grating spectrograph were illuminated in the same way by both the PDL and deuterium lamp, and because the PDL current and pressure were slightly different for the FTS and grating recordings, our resulting intensities should be regarded as approximate and are not recommended for the measurement of branching ratios.

A comparison between the FTS and grating spectra in a small region of overlap is given in Figure 3, which shows that lines observed as blended in the grating spectrum are well resolved in the FTS spectrum.

2.3. Comparison of Wavelengths with Previous Measurements

Our new measurements are not a significant improvement on previous work in the region below 1200 Å where transitions from the $3d^7$ to $3d^64p$ configurations are found. Additional

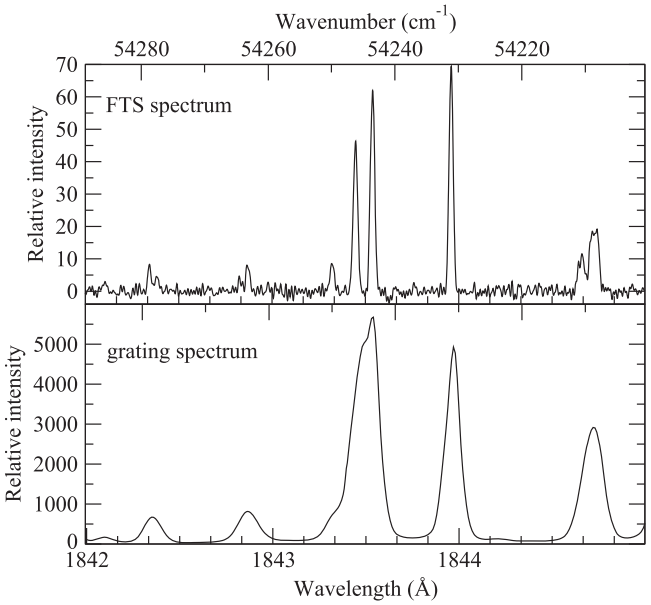

Figure 3. A comparison between the FTS (top) and grating (bottom) spectra for Co III in the wavenumber region 54,200 cm^{-1}–54,290 cm^{-1} (1845.0–1842.0 Å).

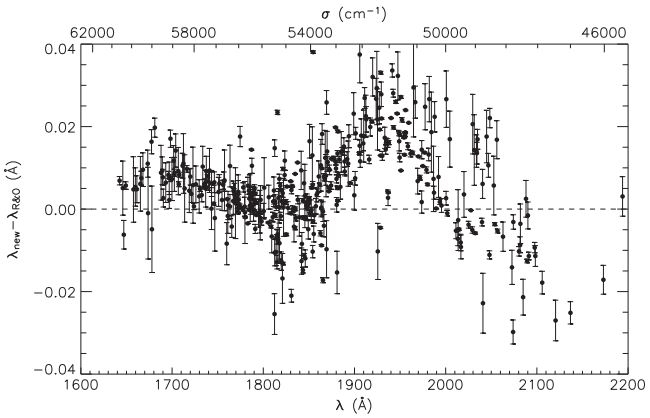

Figure 4. Differences between the FTS Co III wavelengths of this work (λ_{new}) and the wavelengths of R&O ($\lambda_{R\&O}$). The error bars are a sum in quadrature of the joint uncertainties.

lines are also present in the papers of R&O and Shenstone (1960) that we did not observe. Hence in order to optimize all the energy levels using the best available measurements, we have re-evaluated the data of R&O and Shenstone (1960) in order to put their wavelengths on a consistent scale with our new data.

The published wavelengths of R&O and the FTS measurements of this work are compared in Figure 4. Although the wavelength uncertainty quoted in R&O for this region is given as 10 mÅ, the wavelength differences exceed this significantly in many cases and exhibit a striking trend, particularly in the 1850–2000 Å spectral region. Such a trend cannot be present in the FTS spectrum because the wavenumber calibration is simply a wavenumber dependent shift. It is likely that the observed trend in wavenumber differences is due to residuals from the wavelength calibration in the measurements of R&O (Smillie 2007). The wavelengths of R&O between 1412 and 2038 Å were corrected in our level optimization (Section 3.2) by calculating a 50 point running average of the data in Figure 4 and adding that average to R&O's wavelengths. Wavelengths from R&O outside this region were included without change.

The wavelengths of Shenstone (1960) were divided into two regions corresponding to his measurements in air and in vacuum in Table IV of his paper. Nineteen of his lines above 2250 Å correspond to Ritz wavelengths based on energy levels from FTS measurements. Shenstone's wavelengths are smaller than the Ritz wavelengths by 0.04 ± 0.005 Å. We have thus increased Shenstone's wavelengths by 0.04 Å in the level optimization (Section 3.2). Shenstone's wavelengths below 2250 Å agree with the Ritz wavelengths within the uncertainty of 0.02 Å that we have assigned to all of his lines.

3. THE SPECTRUM OF CO III

A section of the list of 754 classified Co III lines is given in Table 1, with the full table available online. Since some spectral lines have more than one plausible classification, Table 1 contains 782 transitions. Where the same line was observed in both the FTS and grating spectra, the values taken are from the FTS measurements. In Table 1, the first column gives the relative intensity of the line measured and calibrated as described in Sections 2.1 and 2.2. The calculated log(gf) values from this work (see Section 3.2) or from Kurucz (2010) are given in the second column. Column 3 gives the full width at half maximum (FWHM, W in Table 1) of the lines taken from the FTS spectrum and is blank for the grating spectra. Columns 4 and 5 contain the observed wavelength and uncertainty (one standard uncertainty). Wavelengths are given in air for wavenumbers below 50,000 cm^{-1} using the five parameter formula of Peck & Reeder (1972). Wavelengths are in vacuum for wavenumbers above 50,000 cm^{-1}. The observed wavenumbers and their uncertainties are given in columns 6 and 7. The Ritz wavelengths and uncertainties, given in columns 8 and 9, were calculated from energy levels optimized with the LOPT program (see Section 3.2). These energy levels, given in columns 10-11, and the classification given in columns 12-13, refer to the energy levels in Table 2. The final column indicates whether the line was taken from the FTS or grating spectra, any blended or doubly identified lines, and additional information relevant to the lines.

3.1. Energy Level Structure

Figure 5 shows the term diagram for Co III incorporating all of the experimentally established energy levels. The boxes represent the distribution of the known energy levels for each subconfiguration. With the exception of the ground configuration, all the known levels are built by adding an electron to one of the terms in Co IV. The ground configuration of Co III is 3d^7. Transitions from this configuration to all the odd-parity levels fall in the vacuum ultraviolet below 1200 Å, a region where our data are not significantly better than R&O. We have thus used the wavelengths of R&O in order to fix the values of the 3d^{6}nl levels with respect to the ground configuration.

The higher levels in Co III fall into three distinct groups. The first group, based on the 3d^6(^{5}D term in Co IV, gives strong lines in our FTS spectrum due to 3d^6(^{5}D)4s–3d^6(^{5}D)4p transitions, enabling accurate *relative* values for all the 3d^6(^{5}D) levels to be found. However, the value of all these levels with respect to the ground configuration is determined by 3d^7–3d^{6}4p transitions in the region below 1200 Å. These spectral lines were taken from R&O and have an uncertainty of about 0.005 Å, with the

Table 1
Observed Lines of Co III (1317–2560 Å)

Int[a]	log(*gf*)[b]	W[c] (mÅ)	Observed[d] Wavelength (Å)	Unc.[e] (Å)	Observed Wavenumber (cm^{-1})	Unc.[e] (cm^{-1})	Ritz[d] Wavelength (Å)	Unc.[e] (Å)	Lower Level (cm^{-1})	Upper Level (cm^{-1})	Classification Lower Level	Classification Upper Level	Notes[f]	
10	−1.67	···	1998.857	0.005	50028.60	0.13	1998.8475	0.0014	89288.021	139316.85	$(^3D)4s\ c^2D_{3/2}$	$(^3D)4p\ x^4P^o_{1/2}$	G	···
91	−0.53	21	1999.7865	0.0009	49989.139	0.021	1999.7863	0.0006	78435.621	128424.767	$(^3P2)4s\ b^2P_{1/2}$	$(^3P2)4p\ y^4D^o_{3/2}$	F	···
18	−1.57	20	2000.066	0.003	49982.14	0.09	2000.06373	0.00023	76520.408	126502.620	$(^3G)4s\ a^4G_{11/2}$	$(^3H)4p\ z^4H^o_{11/2}$	F	···
416	−0.28	29	2001.0846	0.0004	49956.716	0.010	2001.08420	0.00021	76520.408	126477.135	$(^3G)4s\ a^4G_{11/2}$	$(^3H)4p\ z^4H^o_{13/2}$	F	···
10	−1.86	···	2002.160	0.005	49929.89	0.12	2002.1654	0.0003	77122.520	127052.274	$(^3G)4s\ a^4G_{9/2}$	$(^3H)4p\ z^2G^o_{9/2}$	G	···
10	−1.60	···	2002.790	0.005	49914.17	0.12	2002.7976	0.0004	82364.601	132278.596	$(^3G)4s\ b^2G_{9/2}$	$(^3G)4p\ x^4F^o_{7/2}$	G	···
52	−1.05	33	2003.890	0.003	49886.79	0.08	2003.8882	0.0008	85518.751	135405.585	$(^1I)4s\ a^2I_{11/2}$	$(^3G)4p\ z^2H^o_{9/2}$	F	···
30	−1.34	24	2004.272	0.003	49877.27	0.08	2004.2811	0.0005	77122.520	126999.576	$(^3G)4s\ a^4G_{9/2}$	$(^3F2)4p\ y^4F^o_{9/2}$	F	···
9	−1.30	···	2007.280	0.005	49802.55	0.12	2007.2798	0.0009	86328.378	136130.933	$(^1G2)4s\ c^2G_{7/2}$	$(^3G)4p\ y^2F^o_{5/2}$	G	···
16	−1.94	18	2007.472	0.003	49797.79	0.08	2007.4757	0.0006	56794.941	106592.638	$(^5D)4s\ a^4D_{3/2}$	$(^5D)4p\ z^6P^o_{3/2}$	F	···
21	−1.66	···	2008.556	0.005	49770.92	0.12	2008.5560	0.0005	77122.520	126893.436	$(^3G)4s\ a^4G_{9/2}$	$(^3F2)4p\ y^4F^o_{7/2}$	G	···
158	−0.89	30	2010.5917	0.0010	49720.530	0.024	2010.5928	0.0003	76520.408	126240.912	$(^3G)4s\ a^4G_{11/2}$	$(^3H)4p\ z^4I^o_{9/2}$	F	···
691	0.02	29	2011.6212	0.0003	49695.089	0.007	2011.6208	0.0003	77624.280	127319.380	$(^3H)4s\ b^2H_{9/2}$	$(^3H)4p\ z^2G^o_{7/2}$	F	···
120	−0.81	25	2012.7194	0.0009	49667.977	0.021	2012.7193	0.0004	77384.2947	127052.274	$(^3G)4s\ a^4G_{7/2}$	$(^3H)4p\ z^2G^o_{9/2}$	F	···
19	−0.93	22	2013.000	0.004	49661.06	0.09	2013.024	0.003	90913.89	140574.345	$(^1S2)4s\ a^2S_{1/2}$	$(^3D)4p\ y^2P^o_{3/2}$	F	*
794	0.12	24	2013.88151	0.00023	49639.321	0.006	2013.88156	0.00016	77412.9539	127052.274	$(^3H)4s\ b^2H_{11/2}$	$(^3H)4p\ z^2G^o_{9/2}$	F	···
109	−1.20	26	2015.8069	0.0010	49591.91	0.03	2015.8077	0.0005	56373.944	105965.840	$(^5D)4s\ a^4D_{5/2}$	$(^5D)4p\ z^6P^o_{5/2}$	F	···
10	−1.82	11	2015.8906	0.0019	49589.86	0.05	2015.8855	0.0004	76792.604	126382.587	$(^3P2)4s\ b^2P_{3/2}$	$(^3P2)4p\ y^4P^o_{3/2}$	F	*
69	−1.13	25	2016.0218	0.0015	49586.63	0.04	2016.0221	0.0005	77412.9539	126999.576	$(^3H)4s\ b^2H_{11/2}$	$(^3F2)4p\ y^4F^o_{9/2}$	F	···
7	−1.75	···	2016.772	0.005	49568.18	0.12	2016.7524	0.0005	82921.847	132490.517	$(^3G)4s\ b^2G_{7/2}$	$(^3G)4p\ x^4F^o_{5/2}$	G	···

Notes.
[a] Integrated intensity in arbitrary units.
[b] Calculated log(*gf*) value taken from this work unless indicated in last column.
[c] Full width at half maximum in mÅ.
[d] Wavelengths are given in air for wavenumbers below 50,000 cm^{-1} using the five parameter formula of Peck & Reeder (1972). Wavelengths are in vacuum for wavenumbers above 50,000 cm^{-1}.
[e] One standard uncertainty of value in the previous column.
[f] Additional information about the line: F—line measured using FT spectroscopy; G—line measured using grating spectroscopy; II—is a line blended or doubly identified with a Co II line; III—is a line blended or doubly identified with a Co III line; Ne—is a line blended or doubly identified with a neon line; Uk—is a line blended with an unknown line; K—indicates the calculated log(*gf*) is from Kurucz (2010); *—line not used in energy level optimization.

(This table is available in its entirety in machine-readable form.)

Table 2
Co III Energy levels

Designation	J	Level (cm^{-1})	Unc.[a] (cm^{-1})	Unc. gnd[b] (cm^{-1})	No. lines	E_{calc}[c] (cm^{-1})	ΔE[d] (cm^{-1})	Eigenvector Composition (%)[e]	
$3d^7\ a^4F$	9/2	0.00	0.17	0	45	−60	-60	99 %	
	7/2	841.36	0.16	0.19	53	774	−67	99 %	
	5/2	1451.33	0.16	0.19	50	1386	−65	99 %	
	3/2	1867.50	0.19	0.23	37	1804	−63	99 %	
$3d^7\ a^4P$	5/2	15202.56	0.16	0.20	43	15270	67	99 %	
	3/2	15428.57	0.15	0.20	44	15511	82	95 %	+ 4 % $3d^7\ ^2P$
	1/2	15812.37	0.23	0.3	23	15927	114	98 %	+ 2 % $3d^7\ ^2P$
$3d^7\ a^2G$	9/2	16979.56	0.12	0.18	47	16970	−9	97 %	+ 1 % $3d^7\ ^2H$
	7/2	17768.87	0.13	0.19	46	17767	−2	99 %	
$3d^7\ a^2P$	3/2	20197.35	0.15	0.20	39	20172	−25	87 %	+ 6 %$3d^7\ ^2D2$ + 4 % $3d^7\ ^4P$
	1/2	20921.30	0.23	0.24	21	20891	−30	98 %	+ 2 % $3d^7\ ^4P$
$3d^7\ a^2H$	11/2	22721.42	0.24	0.20	30	22801	78	100 %	
	9/2	23435.93	0.15	0.19	39	23510	73	98 %	+ 1 % $3d^7\ ^2G$
$3d^7\ a^2D$	5/2	23060.95	0.13	0.18	47	23138	76	76 %	+ 22 % $3d^7\ ^2D1$
	3/2	24238.81	0.17	0.20	36	24295	55	73 %	+ 18 % $3d^7\ ^2D1$ + 7 % $3d^7\ ^2P$
$3d^7\ a^2F$	5/2	37022.42	0.20	0.19	42	36897	−125	99 %	
	7/2	37317.85	0.15	0.19	41	37253	−65	99 %	
$3d^6(^5D)4s\ a^6D$	9/2	46438.883	0.003	0.14	8	46422	−16	99 %	
	7/2	47003.7239	0.0022	0.14	13	46985	−18	99 %	
	5/2	47416.0161	0.0023	0.14	12	47400	−16	99 %	
	3/2	47699.261	0.005	0.14	10	47686	−13	99 %	
	1/2	47865.356	0.004	0.14	5	47854	−11	99 %	
$3d^6(^5D)4s\ a^4D$	7/2	55729.4633	0.0024	0.14	17	55719	−10	99 %	
	5/2	56373.944	0.003	0.14	17	56374	0	99 %	
	3/2	56794.941	0.003	0.14	15	56806	11	99 %	
	1/2	57037.093	0.006	0.14	8	57055	17	99 %	
$3d^7\ b^2D1$	3/2	57225.6	0.3	0.4	8	57240	14	79 %	+ 20 % $3d^7\ ^2D2$
	5/2	57699.0	0.3	0.3	14	57649	−50	77 %	+ 22 % $3d^7\ ^2D2$

Notes.
[a] Minimum one standard uncertainty of level value with respect to any other level (see text).
[b] One standard uncertainty of level value with respect to ground level.
[c] Calculated value from Cowan code.
[d] Difference between measured and calculated level value.
[e] The symbol * denotes that the level designation is not the largest eigenvector component. † denotes that the level designation is taken from the fourth largest eigenvector component.

(This table is available in its entirety in machine-readable form.)

uncertainty of the energy levels with respect to the ground term of about 0.14 cm^{-1}. Also falling into this group are the $3d^6(^5D)4d$ and $3d^6(^5D)5s$ levels.

The second group of levels is formed by the addition of an electron to the $3d^6$ levels in Co IV and includes levels based on the $^3P2$, ^3H, $^3F2$, ^3G, ^1I, ^3D, $^1G2$, $^1S2$, and $^1D2$ parent terms. Their values can be determined relative to the $3d^6(^5D)4l$ levels by a few weak lines in our FTS and grating spectra with an uncertainty of 0.15 cm^{-1}, but the relative uncertainty of these levels is much smaller and can be as low as 0.002 cm^{-1}.

The third group of levels is based on the $^3P1$, $^3F1$, ^1F, $^1G1$, and $^1D1$ parent terms of the $3d^6$ configuration in Co IV. There are no lines in our FTS spectrum connecting these levels with other $3d^6nl$ levels and only a few, very weak lines in our grating spectra. The relative positions of some of these levels with respect to other levels with the same parent terms can be determined with high accuracy using lines in the FTS spectrum, whereas other levels in these configurations have only weak lines in our FTS spectum. The uncertainties of the latter levels are determined primarily by our grating measurements and those of R&O. The relative values of levels based on the $^1G1$

Table 3
Lines of Co III from Raassen & Ortí Ortin (1984) Used in Level Optimization[a]

Intensity[b]	log(*gf*)[c]	Observed[d] Wavelength (Å)	Unc.[e] (Å)	Waveno. (cm^{-1})	Unc.[e] (cm^{-1})	Ritz Wavelength (Å)	Unc.[e] (Å)	Lower Level (cm^{-1})	Upper Level (cm^{-1})	Classification Lower Level	Classification Upper Level	Notes[f]	
40	−1.01	603.840	0.005	165606.8	1.4	603.8427	0.0007	0.00	165606.05	$3d^7\ a^4F_{9/2}$	$(^3F1)4p\ v^4F^o_{9/2}$	w	*
1	−2.90	605.329	0.005	165199.4	1.4	605.3281	0.0006	0.00	165199.66	$3d^7\ a^4F_{9/2}$	$(^3F1)4p\ v^4F^o_{7/2}$	⋯	⋯
20	−2.03	606.000	0.005	165016.5	1.4	606.0011	0.0006	841.36	165857.56	$3d^7\ a^4F_{7/2}$	$(^3P1)4p\ v^4D^o_{7/2}$	⋯	⋯
3	−3.21	606.134	0.005	164980.0	1.4	606.1359	0.0022	1867.50	166847.0	$3d^7\ a^4F_{3/2}$	$(^3P1)4p\ v^2P^o_{1/2}$	d	*
1	−3.06	606.661	0.005	164836.7	1.4	606.6513	0.0007	1451.33	166290.68	$3d^7\ a^4F_{5/2}$	$(^3P1)4p\ t^2D^o_{3/2}$	⋯	⋯
36	−2.03	606.926	0.005	164764.7	1.4	606.9262	0.0006	841.36	165606.05	$3d^7\ a^4F_{7/2}$	$(^3F1)4p\ v^4F^o_{9/2}$	⋯	⋯
38	−1.41	607.354	0.005	164648.6	1.4	607.3512	0.0006	841.36	165490.75	$3d^7\ a^4F_{7/2}$	$(^3F1)4p\ v^4F^o_{5/2}$	as	*
40	−1.20	608.425	0.005	164358.8	1.4	608.4268	0.0006	841.36	165199.66	$3d^7\ a^4F_{7/2}$	$(^3F1)4p\ v^4F^o_{7/2}$	w	*
36	−1.94	609.607	0.005	164040.1	1.3	609.6096	0.0006	1451.33	165490.75	$3d^7\ a^4F_{5/2}$	$(^3F1)4p\ v^4F^o_{5/2}$	⋯	⋯
37	−2.21	610.459	0.005	163811.2	1.3	610.4614	0.0006	0.00	163810.530	$3d^7\ a^4F_{9/2}$	$(^3F1)4p\ u^2G^o_{9/2}$	⋯	⋯
26	−2.00	610.691	0.005	163748.9	1.3	610.6933	0.0006	1451.33	165199.66	$3d^7\ a^4F_{5/2}$	$(^3F1)4p\ v^4F^o_{7/2}$	⋯	⋯
30	−1.67	610.867	0.005	163701.8	1.3	610.8713	0.0006	1451.33	165151.92	$3d^7\ a^4F_{5/2}$	$(^3F1)4p\ v^4F^o_{3/2}$	⋯	⋯
4	−2.46	611.161	0.005	163623.0	1.3	611.1601	0.0008	1867.50	165490.75	$3d^7\ a^4F_{3/2}$	$(^3F1)4p\ v^4F^o_{5/2}$	⋯	⋯
39	−1.40	611.580	0.005	163510.9	1.3	611.5769	0.0007	1451.33	164963.07	$3d^7\ a^4F_{5/2}$	$(^3P1)4p\ v^4D^o_{5/2}$	⋯	⋯
1	−2.45	611.786	0.005	163455.8	1.3	611.7840	0.0006	841.36	164297.733	$3d^7\ a^4F_{7/2}$	$(^3F1)4p\ u^2G^o_{7/2}$	⋯	⋯

Notes.

[a] Wavenumbers and wavelengths for lines between 1412 and 2038 Å were modified from R&O using Figure 4. Wavelengths and wavenumbers for an additional 714 lines below 1412Å and above 2038Å were not modified.

[b] Intensities taken from R&O are on a different scale to Table 1.

[c] Calculated log(*gf*) value from this work unless indicated in last column.

[d] Wavelengths are given in air for wavenumbers below 50,000 cm^{-1} using the five parameter formula of Peck & Reeder (1972). Wavelengths are in vacuum for wavenumbers above 50,000 cm^{-1}.

[e] One standard uncertainty of the previous column.

[f] Notes are taken from R&O. d—diffuse line; vd—very diffuse line; w—broad line; u—position doubtful; sh—line on shoulder of stronger line; as—asymmetrical, shaded to shorter wavelengths; K—calculated log(*gf*) is from Kurucz (otherwise from this work); *—line not used in the level optimization.

(This table is available in its entirety in machine-readable form.)

Table 4
Lines of Co III from Shenstone (1960) Used in Level Optimization[a]

Intensity[b]	log(*gf*)[c]	Observed[d] Wavelength (Å)	Unc.[e] (Å)	Wavenumber (cm^{-1})	Unc.[e] (cm^{-1})	Ritz[d] Wavelength (Å)	Unc.[e] (Å)	Lower Level (cm^{-1})	Upper Level (cm^{-1})	Classification Lower Level	Classification Upper Level	Notes[f]
20	−0.60	767.703	0.020	130259	3	767.7050	0.0008	841.36	131099.731	$3d^7\ a^4F_{7/2}$	$(^3G)4p\ x^4F^\circ_{9/2}$	⋯
15	−0.40	767.770	0.020	130247	3	767.7802	0.0015	22721.42	152967.03	$3d^7\ a^2H_{11/2}$	$(^1F)4p\ v^2G^\circ_{9/2}$	⋯
20	−0.63	768.456	0.020	130131	3	768.4528	0.0008	1451.33	131582.939	$3d^7\ a^4F_{5/2}$	$(^3G)4p\ x^4G^\circ_{7/2}$	⋯
10	−0.86	769.128	0.020	130017	3	769.1258	0.0011	1867.50	131885.250	$3d^7\ a^4F_{3/2}$	$(^3G)4p\ x^4G^\circ_{5/2}$	⋯
5	−0.68	769.343	0.020	129981	3	769.3508	0.0007	23060.95	153040.66	$3d^7\ a^2D2_{5/2}$	$(^1F)4p\ v^2D^\circ_{5/2}$	⋯
3	−1.38	769.459	0.020	129961	3	769.4567	0.0008	841.36	130803.183	$3d^7\ a^4F_{7/2}$	$(^3F2)4p\ y^2G^\circ_{9/2}$	⋯
1	−1.34	770.192	0.020	129838	3	770.1930	0.0007	16979.56	146817.14	$3d^7\ a^2G_{9/2}$	$(^1D2)4p\ v^2F^\circ_{7/2}$	⋯
2	−0.83	770.723	0.020	129748	3	770.7256	0.0009	37317.85	167065.71	$3d^7\ a^2F_{7/2}$	$(^3P1)4p\ t^2D^\circ_{5/2}$	⋯
0	−1.89	770.967	0.020	129707	3	770.9605	0.0008	0.00	129708.327	$3d^7\ a^4F_{9/2}$	$(^3F2)4p\ y^4G^\circ_{7/2}$	⋯
2	−0.34	1371.419	0.020	72917.2	1.1	1371.409	0.004	98823.641	171741.36	$(^5D)4p\ z^6D^\circ_{5/2}$	$(^5D)5s\ f^6D_{3/2}$	K
0	−0.39	1376.576	0.020	72644.0	1.1	1376.595	0.003	98823.641	171466.63	$(^5D)4p\ z^6D^\circ_{5/2}$	$(^5D)5s\ f^6D_{5/2}$	K
2	−0.28	1378.208	0.020	72558.0	1.1	1378.197	0.004	99182.770	171741.36	$(^5D)4p\ z^6D^\circ_{1/2}$	$(^5D)5s\ f^6D_{3/2}$	K
10	0.12	1378.665	0.020	72533.9	1.1	1378.667	0.004	98546.132	171079.96	$(^5D)4p\ z^6D^\circ_{7/2}$	$(^5D)5s\ f^6D_{7/2}$	K
5	−0.03	1380.775	0.020	72423.1	1.0	1380.782	0.003	99043.919	171466.63	$(^5D)4p\ z^6D^\circ_{3/2}$	$(^5D)5s\ f^6D_{5/2}$	K
20	0.04	1383.971	0.020	72255.8	1.0	1383.962	0.004	98823.641	171079.96	$(^5D)4p\ z^6D^\circ_{5/2}$	$(^5D)5s\ f^6D_{7/2}$	K

Notes.
[a] Wavelengths above 2250 Å were increased by 0.04 Å from Shenstone (1960).
[b] Intensities taken from Shenstone (1960) are on a different scale to Table 1.
[c] Calculated log(*gf*) value taken from this work unless indicated by "K" in last column.
[d] Wavelengths are given in air for wavenumbers below 50,000 cm^{-1} using the five parameter formula of Peck & Reeder (1972). Wavelengths are in vacuum for wavenumbers above 50,000 cm^{-1}.
[e] One standard uncertainty of previous column.
[f] K—calculated log(*gf*) value taken from Kurucz; *—line not used in level optimization.

(This table is available in its entirety in machine-readable form.)

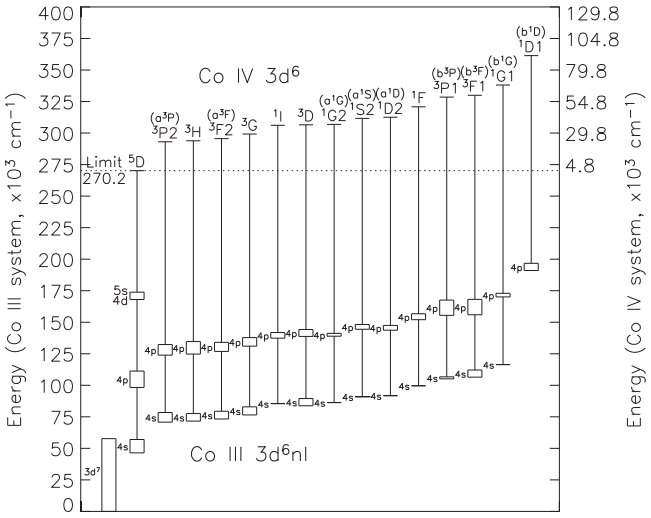

Figure 5. Term diagram of the singly excited system of Co III with the subconfigurations, $3d^6(^ML)nl$, based on the parent terms, ^ML, of the $3d^6$ ground configuration of Co IV, showing the experimentally established energy levels.

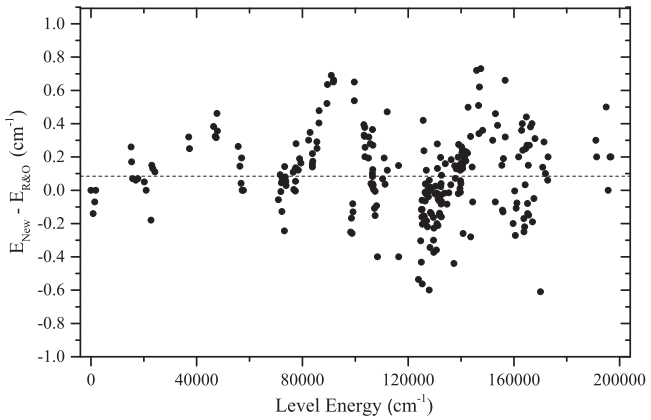

Figure 6. Co III energy level differences between this work, E_{new}, and that of Raassen & Ortí Ortin (1984), $E_{R\&O}$.

Table 5
Fitted and Hartree–Fock (HF) Parameters for the Co III $3d^7$ and $3d^64s$ Configurations

Config. (1)	Parameter (2)	Fitted (cm^{-1}) (3)	HF (cm^{-1}) (4)	Fitted/HF (5)
$3d^7$	E_{av} ($3d^7$)	20669 ± 17	…	…
	F^2(3d,3d)	77082 ± 81	94145	0.819
	F^4(3d,3d)	49457 ± 155	58506	0.845
	α	39.8 ± 2	…	…
	β	678 ± 42	…	…
	$T(3d^7)$	−4.8 (fixed)	…	…
	ζ_{3d}	537 ± 16	538	0.999
4s	E_{av} (4s)	84057 ± 10	56067	1.499
	F^2(3d, 3d)	83222 ± 47	101228	0.822
	F^4(3d, 3d)	52719 ± 98	63231	0.834
	α	39.6 ± 1	…	…
	β	824 ± 26	…	…
	$T(3d^6)$	−5.7 (fixed)	…	…
	ζ_{3d}	607 ± 13	593	1.024
	G^2(3d, 4s)	9240 ± 31	10454	0.884

Note. 77 levels fit with 10 parameters. Mean deviation of fit: 64 cm^{-1}. Standard deviation of fit: 69 cm^{-1}.

Table 6
Fitted and Hartree–Fock (HF) Parameters for the Co III $3d^64p$ Configuration

Config. (1)	Parameter (2)	Fitted (cm^{-1}) (3)	HF (cm^{-1}) (4)	Fitted/HF (5)
4p	E_{av} (4p)	138302 ± 13	…	…
	F^2(3d, 3d)	84395 ± 59	101677	0.830
	F^4(3d, 3d)	52705 ± 208	63535	0.830
	α	41.9 ± 3	…	…
	β	838 ± 51	…	…
	$T(3d^6)$	−5.7 (fixed)	…	…
	ζ_{3d}	631 ± 22	595	1.060
	ζ_{4p}	707 ± 38	599	1.180
	F^2(3d, 4p)	17041 ± 105	18676	0.912
	G^1(3d, 4p)	6071 ± 58	6805	0.892
	G^3(3d, 4p)	4613 ± 108	5904	0.781

Note.178 levels fit with 11 parameters. Mean deviation of fit: 158 cm^{-1}. Standard deviation of fit: 164 cm^{-1}.

parent are determined well by FTS lines, but are connected to other levels only through 3d–4p transitions taken from R&O. No lines from levels based on the ^{1}D1 parent are observed in our spectra and the levels in Table 2 are based solely on 3d–4p transitions taken from R&O.

3.2. Level Optimization

The Penning discharge source generates spectra of Co I–III and Ne I–III. Identification of Co I and Co II lines in our line list was carried out using Ritz wavelengths from the energy levels of Pickering (1994, 1998), Pickering & Thorne (1996), and Pickering et al. (1998). Neon lines were identified using Ralchenko et al. (2007), which includes the work of Saloman & Sansonetti (2004) (Ne I), Kramida & Nave (2006a) (Ne II), and Kramida & Nave (2006b) (Ne III).

Co III lines were identified using 287 energy levels from R&O and Shenstone (1960). The $f^6D_{1/2}$ level from Shenstone (1960) was established by only one weak line. Since two other lines from this level are predicted to be stronger, but are not present in either Shenstone's list or our list, this level has been discarded. The remaining levels were optimized to the observed lines using the Lopt computer program of Kramida (2011). In addition to our new measurements, we included 790 lines from R&O and 87 lines from Shenstone (1960) that are not present in our spectra. Since some of these lines have more than one plausible classification, these lines give 815 transitions and 90 transitions, respectively. The wavelengths of R&O were adjusted to put them on the same scale as given in Section 2.3. The lines taken from R&O are listed in Table 3. Wavelengths of the 87 lines taken from Shenstone (1960) were adjusted as in Section 2.3 and are listed in Table 4. Blended and multiply classified lines were included in the level fitting procedure but were given a low weight, as were lines marked as diffuse, asymmetrical, hazy, or otherwise doubtful in R&O or Shenstone (1960). Over 60% of the revised levels have uncertainties that are an order of magnitude or more lower than previous measurements.

Figure 6 shows the differences in energy between the improved energy levels of this work and those of R&O plotted against level energy, with the striking pattern in these differences reflecting the issues with wavelength calibration

Table 7
Ritz Wavelengths of Forbidden Lines in Co III

Lower[a] Term	Upper[a] Term	Ritz Air Wavelength (Å)	Ritz Vacuum Wavelength (Å)	Unc.[b] (Å)	Ritz Waveno. (cm^{-1})	Unc.[b] (cm^{-1})	Lower Level (cm^{-1})	Upper Level (cm^{-1})	A-value[c] (s^{-1})	Type[d]
$a^4F_{9/2}$	$b^2D_{5/2}$		1733.132	0.008	57699.0	0.3	0.00	57699.0	0.039	E2
$a^4F_{3/2}$	$b^2D_{5/2}$		1758.779	0.008	56857.6	0.3	841.36	57699.0	0.11	E2+M1
$a^4F_{3/2}$	$b^2D_{3/2}$		1773.545	0.012	56384.2	0.4	841.36	57225.6	0.0076	E2
$a^4F_{5/2}$	$b^2D_{5/2}$		1777.851	0.008	56247.7	0.3	1451.33	57699.0	0.019	E2+M1
$a^4F_{3/2}$	$b^2D_{5/2}$		1791.104	0.009	55831.5	0.3	1867.50	57699.0	0.0085	E2+M1
$a^4F_{5/2}$	$b^2D_{3/2}$		1792.941	0.012	55774.3	0.4	1451.33	57225.6	0.13	M1
$a^4F_{3/2}$	$b^2D_{3/2}$		1806.420	0.013	55358.1	0.4	1867.50	57225.6	0.085	M1
$a^4P_{5/2}$	$b^2D_{5/2}$	2352.418	2353.138	0.014	42496.4	0.3	15202.56	57699.0	0.86	M1
$a^4P_{3/2}$	$b^2D_{5/2}$	2364.997	2365.720	0.014	42270.4	0.3	15428.57	57699.0	0.26	E2+M1
$a^4P_{5/2}$	$b^2D_{3/2}$	2378.921	2379.647	0.022	42023.0	0.4	15202.56	57225.6	0.11	M1
$a^4P_{3/2}$	$b^2D_{5/2}$	2386.669	2387.397	0.017	41886.6	0.3	15812.37	57699.0	0.01	E2
$a^4P_{3/2}$	$b^2D_{3/2}$	2391.786	2392.514	0.022	41797.0	0.4	15428.57	57225.6	0.38	E2+M1
$a^4P_{3/2}$	$b^2D_{3/2}$	2413.953	2414.687	0.024	41413.2	0.4	15812.37	57225.6	0.11	E2+M1
$a^2G_{9/2}$	$b^2D_{5/2}$	2455.086	2455.829	0.015	40719.44	0.24	16979.56	57699.0	6.4	E2
$a^2G_{7/2}$	$b^2D_{5/2}$	2503.620	2504.375	0.015	39930.13	0.25	17768.87	57699.0	0.46	E2
$a^2G_{7/2}$	$b^2D_{3/2}$	2533.660	2534.422	0.024	39456.7	0.4	17768.87	57225.6	6.4	E2
$a^2P_{3/2}$	$b^2D_{5/2}$	2665.757	2666.549	0.018	37501.7	0.3	20197.35	57699.0	1.7	E2+M1

Notes:
[a] Term of the $3d^7$ configuration.
[b] One standard uncertainty of the previous column.
[c] Transition rate taken from Hansen et al. (1984)
[d] E2+M1 if minor contribution is more than 2% of total.

(This table is available in its entirety in machine-readable form.)

in the work of R&O as discussed in Section 2.3 and seen in Figure 4. Ritz wavenumbers were generated from the revised levels using the Lopt program for all the lines included in the level optimization.

The revised Co III energy levels are presented in Table 2. Calculations of the energy level structure and $\log(gf)$ values were carried out using the Cowan code (Cowan 1981) for the $3d^7$, $3d^64s$, and $3d^64p$ Co III configurations, and the results are generally in good agreement with similar calculations performed by R&O. The calculated level energies and eigenvector percentage compositions are also presented in Table 2. Calculated $\log(gf)$ values are given in the second column of Table 1; if not calculated in this work, values from Kurucz (2010) are given instead. These were mainly for the $3d^6$ 4d and $3d^6$ 5s configurations, which were not included in our calculations. The calculated $\log(gf)$ values were useful as additional confirmations of the line classifications.

Our optimized energy level values for these levels are given in column 3 of Table 2, with the level designation and J value in columns 1 and 2, respectively. Two uncertainties are given for the energy level values. The first, in column 4, is the minimum uncertainty with respect to any of the other levels. This is the most appropriate uncertainty to use when deriving Ritz wavelengths of spectral lines that are not included in our table, where both energy levels originate from the same or similar parent terms. The second uncertainty in column 5 is the uncertainty of the level with respect to the ground level. Details of how these uncertainties are calculated are given in Kramida (2011). The number of lines combining with the level is given in column 6. Columns 7 and 8 give the level value obtained from the Cowan code calculations and its difference from the experimental value. The final column gives the calculated eigenvector percentage compositions for the most significant components, unless indicated otherwise. From the Cowan code calculations, the least squares fitted and Hartree–Fock parameters, E_{av}, the average energies for the configurations, F^k and G^k, the Slater integrals (exchange parameters), ζ_k, the spin–orbit parameters, and effective parameters α, β, and T (see Hansen & Raassen 1981), are given in Tables 5 and 6, for the $3d^7$ and $3d^64s$, and $3d^64p$ configurations, respectively. Initial values for the α, β, and T parameters were taken from R&O with the T parameter fixed. The leading percentages for the energy levels from the $3d^7$ and $3d^64s$ configurations agree closely with those calculated by R&O, with the lowest leading percentage for any of these levels of 60%. In general, the leading percentages for the $3d^64p$ configurations are comparable to those calculated by R&O. Many of the $3d^64p$ levels are highly mixed, with the LS coupling level designation sometimes not representative of the energy level nature.

Forbidden lines can be important diagnostics of astrophysical plasmas but are rarely observed in laboratory plasmas of low ionization stages. However, accurate wavelengths for forbidden lines can be derived in our level optimization. We selected 98 lines from Hansen et al. (1984) with transition rates greater than 0.001 s^{-1} and derived Ritz wavelengths for them using Lopt. These lines are presented in Table 7, together with the calculated transition rates from Hansen et al. (1984).

4. SUMMARY

Accurate laboratory measurements of the doubly ionized iron group element spectra are urgently needed for analysis of high resolution spectra of hot B stars. Previous measurements of the Co III spectrum have used grating spectrometers, with typical wavelength uncertainties in the range 5–10 mÅ, although uncertainties as low as 0.2 mÅ at 2000 Å are required for analysis of state of the art stellar spectra. This work has presented the first high resolution FTS measurements of the Co III spectrum, with 514 classified lines in the region 1562–2564 Å (64,000–39,000 cm^{-1}). The wavenumber uncertainties (one standard uncertainty) of the Co III lines in our FTS spectra are as low as 0.004 cm^{-1} (approximately 0.2 mÅ at 2000 Å, or 1 part in 10^7) for the strongest isolated lines, more than an order of magnitude improvement in accuracy over previous measurements. The FTS measurements were supplemented by grating spectra recorded using the NIST NIVS with image plate detectors, providing a further 240 classified lines in the region 1317–2500 Å (75,905–40,000 cm^{-1}) with estimated wavelength uncertainties of 5 mÅ. The new term analysis using the FTS and grating lines has led to reduced uncertainties of the energy level values for all but one of the 288 Co III energy levels assigned in R&O, providing Ritz wavelengths for all the measured lines and an additional 877 allowed lines and 98 forbidden lines from previous work. Order of magnitude improvements in accuracy were obtained for over 60% of the revised levels.

This work was supported in part by NASA grant NAG5-12668, NASA inter-agency agreements W-10,255 and NNH10AH38I, the STFC and PPARC (UK), the Royal Society of the UK, and by the Leverhulme Trust.

REFERENCES

Ayres, T. R. 2013, AN, 334, 105
Cowan, R. D. 1981, The Theory of Atomic Structure and Spectra (Berkeley, CA: Univ. California Press)
Cowley, C. R., & Frey, M. 1988, NIMPB, B31, 214
Davis, S. P., Abrams, M. C., & Brault, J. W. 2001, Fourier Transform Spectrometry (New York: Academic)
Griesmann, U., Kling, R., Burnett, J. H., Bratasz, L., & Gietzen, R. A. 1999, Proc. SPIE, 3818, 180
Hansen, J. E., & Raassen, A. J. J. 1981, PhyC, 111, 76
Hansen, J. E., Raassen, A. J. J., & Uylings, P. H. M. 1984, ApJ, 277, 435
Heise, C., Hollandt, J., Kling, R., Kock, M., & Kühne, M. 1994, ApOpt, 33, 5111
Hollandt, J., Becker, U., Paustian, W., Richter, M., & Ulm, G. 2000, Metro, 37, 563
Iglesias, L. 1979, Opt. Pur. Y Apl., 12, 63
Iwabuchi, Y., Mori, N., Takahashi, K., Matsuda, T., & Shionoya, S. 1994, JaJAP, 33, 178
Johansson, S. 1987, PhyS, 36, 99
Johansson, S. 1996, PhST, T65, 7
Katto, M., Matsumoto, R., Kurosawa, K., et al. 1993, RScI, 64, 319
Kramida, A. E. 2011, CoPhC, 182, 419
Kramida, A. E., & Nave, G. 2006a, EPJD, 39, 331
Kramida, A. E., & Nave, G. 2006b, EPJD, 37, 1
Kurucz, R. L. 2010, [Online] Available: http://kurucz.harvard.edu [2010, August]
Leckrone, D. S., Johansson, S., Wahlgren, G. M., Proffitt, C. R., & Brage, T. 1996, PhST, T65, 110
Moore, C. E. 1952, Nat. Bur. Std. (U.S.), Circ. 467 II
Murray, J. E. 1992, PhD thesis, Imperial College London
Nave, G., Griesmann, U., Brault, J. W., & Abrams, M. C. 2015, ascl, ascl: 1511.004
Nave, G., & Johansson, S. 2013, ApJS, 204, 1
Nave, G., Johansson, S., Learner, R. C. M., Thorne, A. P., & Brault, J. W. 1994, ApJS, 94, 221
Nave, G., & Sansonetti, C. J. 2011, JOSAB, 28, 737
Nave, G., Sansonetti, C. J., & Griesmann, U. 1997, Opt. Soc. Am. Tech. Dig., 3, 38
Nave, G., Sansonetti, C. J., Szabo, C. I., Curry, J. J., & Smillie, D. G. 2011, RScI, 82, 013107
Norlén 1973, PhyS, 8, 249
Pasternak, A., & Goldschmidt, Z. B. 1972, PhRvA, 6, 55
Peck, E. R., & Reeder, K. 1972, Opt. Soc. AM, 62, 958
Pickering, J. C. 1994, PhD thesis, Imperial College London
Pickering, J. C. 1998, PhyS, 57, 385
Pickering, J. C. 2002, Vib. Spec., 29, 27
Pickering, J. C., Raassen, A. J. J., Uylings, P. H. M., & Johansson, S. 1998, ApJS, 117, 261
Pickering, J. C., & Thorne, A. P. 1996, ApJS, 107, 761
Raassen, A. J. J., & Ortí Ortin, S. 1984, PhyC, 123, 353
Ralchenko, Yu., Jou, F.-C., Kelleher, D. E., et al. 2007, National Institute of Standards and Technology Atomic Spectra Database (version 3.1.2), [Online] Available: http://physics.nist.gov/asd3 [2007, August]
Reader, J., Feldman, U., & Brown, C. M. 2006, ApOpt, 45, 7657
Roth, C. 1968, JRNBS, 72A, 505
Saloman, E. B., & Sansonetti, C. J. 2004, JPCRD, 33, 1113
Shenstone, A. G. 1960, CaJPh, 38, 677
Smillie, D. G. 2007, PhD thesis, Univ. London
Smillie, D. G., Pickering, J. C., & Smith, P. L. 2008, MNRAS, 390, 733
Smillie, D. G., Pickering, J. C., Smith, P. L., Nave, G., & Blackwell-Whitehead, R. J. 2006, in Proc. 2006 NASA Lab. Astrophys. Workshop (NASA/CP-2006-214549), ed. P. F. Week, V. H. S. Kwang, & F. Salama (Moffet Field, CA: Ames Research Center), 256
Smith, P. L., Thorne, A. P., Learner, R. C. M., et al. 1998, in ASP Conf. Ser. 143, The Scientific Impact of the Goddard High Resolution Spectrograph, ed. J. C. Brandt, T. B. Ake, & C. C. Peterson (San Francisco, CA: ASP), 395
Sugar, J., & Corliss, C. 1985, JPCRD, 14, 529
Swings, J. P., Klutz, M., & Vreux, J. M. 1976, A&AS, 25, 193
Thorne, A. P., Pickering, J. C., & Semeniuk, J. I. 2011, ApJ, 192, 11
Thorne, A. P., Pickering, J. C., & Semeniuk, J. I. 2013, ApJ, 207, 13
Vizbaraite, J., Kupliauskis, Z., & Tutlys, V. 1968, LFR, 8, 497
Whaling, W., Anderson, W. H. C., Carle, M. T., Brault, J. W., & Zarem, H. A. 1995, JQSRT, 53, 1